

RESONANCE LIGHT-SCATTERING ENHANCEMENT EFFECT OF THE Y(III)–PUFX–EOSIN SYSTEM AND ITS FLUORESCENCE STUDY

Shaista Bano,^{1,*} Ayaz Mohd,^{1,2} Aftab Aslam Parwaz Khan,³
Abdullah M. Asiri,³ Jamal Akhter Siddiqui,⁴ and Siti Aslina Hussain¹

Original article submitted November 21, 2017.

Highly sensitive and rapid method for the determination of prulifloxacin (PUFX) has been developed on the basis of ion association reaction of PUFX, Y(III) and eosin Y (EY). In pH 6.5 BR buffer medium, PUFX reacts with Y(III) to form a 2:1 cationic chelate which further reacts with EY to form 2:1 ion-association complex. As a result, not only the spectra of absorption are changed, but quenching of fluorescence and significant enhancement of resonance Rayleigh scattering (RRS) is observed. Furthermore, a new RRS spectrum would appear, and the maximum RRS wavelength was located at about 375 nm. The fluorescence quenching (FQ) and enhanced RRS intensity were directly proportional to the PUFX concentration in the ranges of $1.5 - 7.6 \mu\text{g mL}^{-1}$ and $0.004 - 3.0 \mu\text{g mL}^{-1}$ with detection limits 8.5 ng mL^{-1} and 1.1 ng mL^{-1} , respectively. The optimum conditions of RRS method and the effects of coexisting substances on the reaction were investigated. In addition the composition of ion-association complexes, the reaction mechanism, the energy transfer between absorption, fluorescence and RRS and reasons for RRS enhancement were discussed. The methods were applied to the determination of PUFX in pharmaceutical samples with satisfactory results.

Keywords: prulifloxacin; resonance Rayleigh scattering enhancement; fluorescence spectrometry; antibiotics.

1. INTRODUCTION

Prulifloxacin (PUFX), or (\pm) -6-fluoro-1-methyl-7-[4-(5-methyl-2-oxo-1,3-dioxolen-4-yl)methyl-1-piperazinyl]-4-oxo-4H-[1,3]thiazeto[3, 2-a]quinoline-3-carboxylic acid (Fig. 1), is the prodrug of ulifloxacin. It belongs to the class of fourth-generation synthetic fluoroquinolone antibiotics with broad-spectrum *in vitro* activity against various Gram-negative and Gram-positive bacteria, which acts directly on bacterial DNA gyrase inhibiting cell reproduction that leads to cell death [1]. PUFX contains a quinolone skele-

ton with a four-member ring in 1,2-position, including a sulfur atom to increase antibacterial activity and anoxodioxolonylmethyl group in the 7-piperazine ring to improve oral absorption. After oral administration, prulifloxacin is absorbed in the intestine and enters the circulation, where it is immediately and quantitatively transformed into its active metabolite ulifloxacin [2], and other metabolites accounting for 15% of the administered dose [3].

Several methods have been reported for the determination of PUFX, including HPLC coupled with UV detection [4], fluorescence detection [5] and mass spectrometry [6], headspace capillary gas chromatography [7], capillary electrophoresis [8], spectrofluorimetry [9, 10], and chemiluminescence [11, 12, 13]. Among these, HPLC has good sensitivity, accuracy, and precision, but sample processing is complicated, the analytical condition is harsh, and the instrumentation is expensive. The method of headspace capillary gas chromatography also has some limitations since running of equipment is costly and life span is short. To overcome these disadvantages, other methods such as fluorimetry and chemiluminescence have been developed, but these methods have somewhat insufficient sensitivity or selectiv-

¹ Department of Chemical and Environmental Engineering, Faculty of Engineering, Universiti Putra Malaysia, 43400 Serdang, Selangor, Malaysia.

² Ministry of Higher Education, Applied Biotechnology Department, Sur College of Applied Sciences, P. O Box: 484, Postal Code: 411, Sur-Sultanate of Oman.

³ Center of Excellence for Advanced Materials Research and Chemistry Department, Faculty of Science, King Abdulaziz University, Jeddah 21589, P. O. Box 80203, Saudi Arabia.

⁴ Department of Materials Engineering and Chemistry, Faculty of Civil Engineering, Czech Technical University (CVUT), Prague Thakurova 7, 16629 Praha 6, Czech Republic.

* e-mail: shaistairfan@yahoo.com

ity. The fluorimetric techniques are mainly based on complexation with Al(III), Y(III) and Tb(III). However the sensitivity is not high enough as the detection limits range from 8.5×10^{-9} to 2×10^{-8} M. Therefore, it is necessary to develop new and fast spectral methods with high sensitivity, good selectivity and simplicity to determine PUFX traces.

Resonance Rayleigh scattering (RRS), as a sensitive and simple detection technique, has been applied to determine macromolecules such as nucleic acids [14], proteins [15], heparin [16], metal ions [17], non-metal ions [18], and organic compounds [19]. In recent years, RRS has been increasingly used in drug analysis [20–22]. To the best of the authors' knowledge, the use of resonance Rayleigh scattering (RRS) technique for determining PUFX has not been reported until now.

In the present study, a new approach was investigated and novel, highly sensitive and simple fluorescence quenching (FQ) and RRS methods have been proposed for the determination of PUFX traces. These methods are based on the formation of a ternary complex of Y(III), PUFX and EY. In this work, the spectral characteristics of Y(III)–PUFX–EY ternary ion-association complexes, optimum reactions, and related influencing factors have been investigated. The effects of foreign substances were also examined. In addition, the composition of the ternary ion-association complex was investigated, and the structure of the complex and its reaction mechanisms were considered.

2. EXPERIMENTAL PART

2.1. Instrumentation and Reagents

A Hitachi F-2500 spectrofluorophotometer (Tokyo, Japan) was used for measuring the RRS intensities with the slits (Ex/Em) of 5.0/5.0 nm. An Elico-SL-169 double-beam UV-VIS spectrophotometer was used for recording the absorption spectra and Elico-LI-120 pH meter was used for measuring pH.

The concentration of PUFX stock solution (Ranbaxy Laboratories Ltd.) was $100 \mu\text{g mL}^{-1}$ and the concentration of working PUFX solution was $40 \mu\text{g mL}^{-1}$. EY (EV, Gurr), DIF (MV, Shanghai Specimen and Model Factory, China), Ery (CV, Chongming Chemistry Reagent Factory, China) working solutions were all prepared as 2.0×10^{-4} mol L⁻¹. The solution of Y(III) (2.0×10^{-2} M) was prepared by dissolving Y₂O₃ (purity, 99.99%) in 1:1 HCl, evaporating the solution to almost dryness, and final diluting to 100 mL with water. The working standard solutions were prepared by making appropriate dilutions with water. Britton–Robinson (BR) buffer solutions with various pH were prepared by mixing acids (mixture composed of 0.04 M H₃PO₄, HAc and H₃BO₃) with 0.2 M NaOH in necessary proportion. The pH values were adjusted with the aid of a pH meter. All reagents were of analytical-grade and doubly distilled water was used throughout.

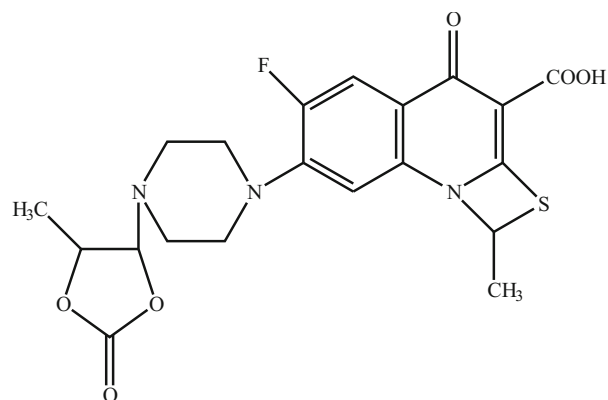


Fig. 1. Chemical structure of PUFX.

2.2. General Procedure

Aliquot (1.0 mL) of pH 6.4 BR solution was placed in a 10.0 mL calibrated flask, followed by 0.2 mL of 1.4×10^{-4} M halofluorescein dye, 2 mL of 1×10^{-5} M Y(III) solution, and suitable amount of PUFX solution. The mixture was diluted to the mark with water, shaken thoroughly, and allowed to stand for 15 min. The RRS spectra of the systems were recorded with synchronous scanning as $\lambda_{\text{ex}} = \lambda_{\text{em}} (\Delta\lambda)$. The sample and reagent blank scattering intensities (I_{RRS} and I_{RRS}^0) were measured spectra of at their own maximum scattering wavelength, $\Delta I_{\text{RRS}} = I_{\text{RRS}} - I_{\text{RRS}}^0$. The optical absorption and fluorescence spectra were recorded simultaneously

3. RESULTS AND DISCUSSION

3.1. RRS Spectra

The RRS spectra of Y(III)-PUFX-halofluorescein dye (HFD) systems are shown in Fig. 2. It can be seen that RRS intensities of PUFX, HFDs such as diiodofluorescein (DIF), erythrosine (Ery) and eosin Y (EY) themselves are very weak, and binary Y(III)–PUFX chelates can only result in little enhancement of RRS intensities. When these binary chelates further react with HFD to form ternary complexes, RRS intensities are enhanced greatly. The three reaction products have similar spectral characteristics as the maximum RRS peaks are all at 375 nm and the other smaller peaks are located at 570 nm. The enhancement of I_{RRS} at 375 nm is larger than that at 570; therefore, 375 nm was selected for further research. The intensities of reaction products are different and the order of their intensities is $\text{EY} > \text{Ery} > \text{DIF}$. Therefore, EY as the most sensitive probe was selected for further studies. It can be seen that the enhancement in RRS intensity for Y(III)-PUFX-EY system is proportional to the concentrations of PUFX in a certain range (Fig. 3). Hence, the RRS method can be applied for the determination of PUFX.

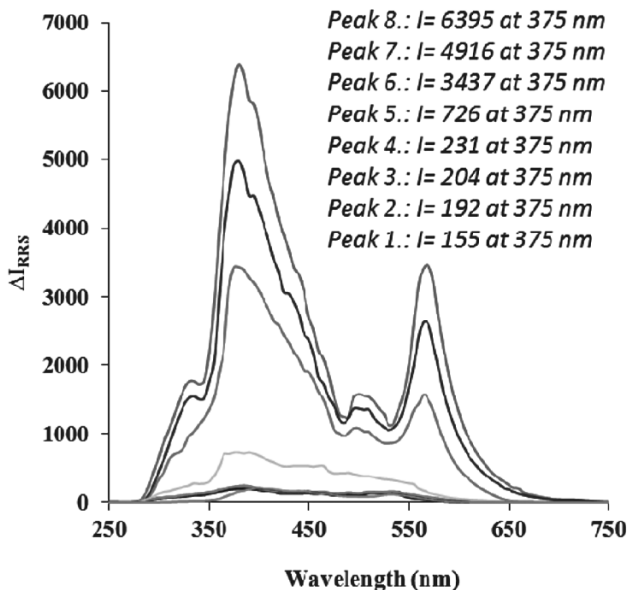


Fig. 2. RRS spectra of Y(III)-PUFX-HFD systems: (1) DIF; (2) ERY; (3) EY; (4) PUFX; (5) Y(III)-PUFX; (6) Y(III)-PUFX-DIF; (7) Y(III)-PUFX-ERY; (8) Y(III)-PUFX-EY. Concentration: [PUFX] = 3.5 $\mu\text{g/mL}$; [DIF, ERY, EY] = 2.8×10^{-5} M; [Y(III)] = 2.0×10^{-5} M.

3.2. Optimum Reaction Conditions

Effect of pH. The effect of pH on the RRS intensity in the system is shown in Fig. 4. It can be seen that RRS intensity increases with increasing pH, reached a maximum between pH 6 and 6.6, and then sharply decreases. Thus, pH 6.4 was selected for subsequent experiments. The decrease in RRS intensity may be caused by Y(III) ion deposited in a strong alkaline medium, which blocked the coordination between PUFX and Y(III) ion. Experiments indicated that the buffer had a large effect on the RRS intensity. Several buffers were tested, including the following: HAc-NaAc, borax-HCl, NaHPO_4 -HCl, KH_2PO_4 -NaOH, phthalate-NaOH, and BR. The results indicated that BR was the best buffer of those tested. Thus, BR buffer (pH 6.4) was selected for the assay, and the optimum volume of BR buffer was 1.0 mL.

Effect of eosin concentration. The suitable concentration of EY (Fig. 5) was between 1.2×10^{-5} mol L^{-1} and 3.5×10^{-5} mol L^{-1} . If the concentration of EY was below 1.2×10^{-5} mol L^{-1} , the reaction could be incomplete. On the contrary, if the EY concentration was higher than 3.5×10^{-5} mol L^{-1} , the RRS intensity could decrease because of the formation of EY dimers by self-aggregation. Thus, 2.8×10^{-5} mol L^{-1} was chosen as the EY reaction concentration.

Effect of Y(III) concentration. The effect of Y(III) concentration on RRS intensities of Y(III)-PUFX-EY systems is illustrated in Fig. 6. It can be seen that RRS intensity reached maximum and remained stable when the concentration of

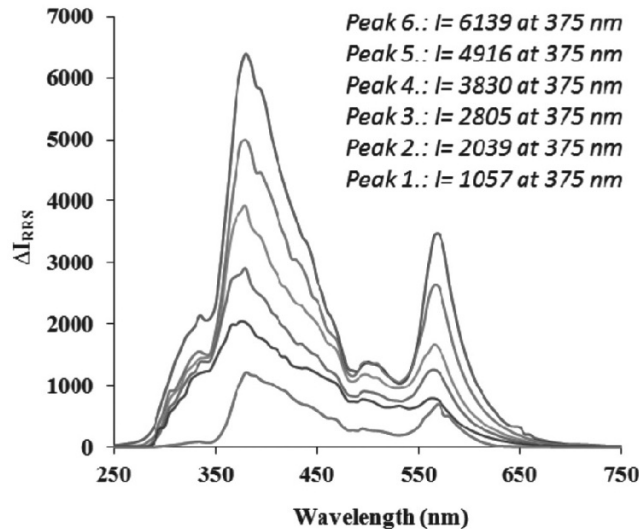


Fig. 3. RRS spectra of Y(III)-PUFX-EY system with PUFX concentrations 0.003, 0.1, 0.8, 1.2, 1.7, 2.8 and 3.6 $\mu\text{g/mL}$ (curves 1 to 7, respectively).

Y(III) was within 1.5×10^{-5} – 2.5×10^{-5} M, and then gradually decreased with further increase in the Y(III) concentration. Thus, the experimental concentration of Y(III) was selected at 2×10^{-5} M.

Effect of ionic strength. The effect of ionic strength on the RRS intensity was investigated with NaCl solutions. The results showed that, when the NaCl concentration was below 4.0×10^{-2} M, I_{RRS} kept constant and then gradually decreased with increasing NaCl concentration. Thus, the ion-association reaction should be carried out under a low ionic strength condition. The results also indicated that the electrostatic interaction was very important factor in this ion-association reaction. When the concentration of NaCl increases, electrostatic shielding of charges reduces the formation of Y(III)-PUFX-EY complexes.

Reaction velocity and stability. At room temperature, the reaction finished in 15 min and the RRS intensity reached maximum at the same time. Then, the RRS signal remained constant for 3 h at least.

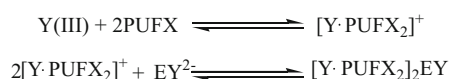
3.3. Sensitivity of the Proposed Methods

Under the optimum conditions, various concentrations of PUFX reacted with Y(III) and EY to form ternary complex and the intensities ΔI_{RRS} and ΔF were separately measured at their maximum scattering wavelengths after 15 min. The calibration graphs of ΔI_{RRS} and ΔF against the PUFX concentration were constructed. The linear regression equations, correlation coefficients, linearity ranges, and detection limits are listed in Table 1. It can be seen from the table that both the methods have high sensitivity with detection limits (3σ) 1.29 ng mL^{-1} for RRS and 8.5 ng mL^{-1} for FQ. Thus, the

RRS method has much higher sensitivity than other common analytical techniques (Table 2).

3.4. Structure of Complexes and Reaction Mechanism

The composition ratio of binary chelate for the Y(III)-PUFX system and ternary complex for Y(III)-PUFX-EY system was established by using Job's method of continuous variation. It is shown that the composition ratio is 1:2 for Y(III)-PUFX and 2:4:1 for Y(III)-PUFX-EY that is, the composition of ternary ion-association complex is $[Y \cdot PUFX_2]_2EY$. The structure of the complex and reaction mechanism is as follows:



Thus, Y(III) can react with PUFX to form 1:2 cationic chelate $[Y \cdot PUFX_2]^+$.

There are two types of coordinating atoms in the molecule of PUFX: nitrogen and oxygen. The oxygen atom tends to form a stable complex with rare-earth element, due to its strong ability of coordination to rare earths. On the other hand, the stability of a complex formed by nitrogen atom and a rare earth is relatively poor. Usually, oxygen atoms in an organic ligand coordinate with the rare earth in two ways, the negatively charged oxygen atom forming a stable ionic bond with the rare-earth ion and the electroneutral oxygen atom forming coordinate bonds with the rare-earth ion [23]. Based on the above discussion, a structure of the formed complex has been proposed that is shown in Fig. 7.

In aqueous solutions, EY exists in the form of species such as H_3L^+ , H_2L^+ , HL^- and L^{2-} . According to the dissociation constant of EY ($pK_{a1}=2.10$, $pK_{a2}=2.85$, $pK_{a3}=4.95$) [24], the dominant species of EY at pH 6.4, is L^{2-} , which can react with $[Y \cdot PUFX_2]^+$ to form a ternary ion-association complex through electrostatic attraction and hydrophobic forces. The structure of $[Y \cdot PUFX_2]_2EY$ is shown in Fig. 7.

3.5. Effect of the Ion-Association Reaction on Spectral Characteristics of Complexes

Effect on absorption spectra. It can be seen that PUFX has a maximum absorption peak (λ_{max}) at 280 nm (Fig. 8). When Y(III) was added, the maximum absorption peak of PUFX underwent a blue shift from 280 nm to 275 nm with an appreciable increase in absorbance and a new peak is appeared at 350 nm with molar absorptivity $4.4 \times 10^4 \text{ L mol}^{-1}$

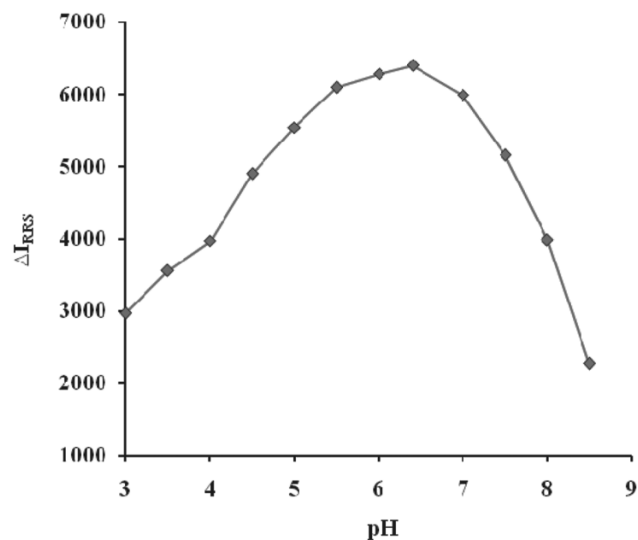


Fig. 4. Effect of pH on I_{RRS} in Y(III)-PUFX-EY systems at 375 nm. Concentrations: $[PUFX] = 3.0 \mu\text{g mL}^{-1}$; $[Y(III)] = 2.0 \times 10^{-5} \text{ M}$; $[EY] = 2.8 \times 10^{-5} \text{ M}$.

cm^{-1} indicating the formation of Y(III)-PUFX complex. This signal could not be used for the determination of PUFX by spectrophotometry. When this binary complex further reacts with EY to form ternary ion-association complex, a new absorption peak appears at about 530 nm, but the sensitivity is still not high with molar absorptivity $4.4 \times 10^4 \text{ L mol}^{-1} \text{ cm}^{-1}$. Therefore it is not advantageous to determine PUFX by spectrophotometry.

Effect on fluorescence spectra. EY has strong fluorescence at maximum excitation (λ_{ex}) and emission (λ_{em}) wavelengths of 515 nm and 540 nm, respectively. When EY reacts with $[Y \cdot PUFX_2]^+$, the dissociative EY concentration decreases that leads to the FQ and the quenching intensity is directly proportional to the concentration of PUFX in a certain range (Fig. 9). The FQ method is highly sensitive. The detection limit is 8.5 ng mL^{-1} , which is lower than that of existing fluorimetric techniques [9–11]. Therefore, the reaction of ternary ion-association can be applied to determine PUFX by the proposed FQ method.

3.6. Reasons for RRS Intensity Enhancement

Effect of absorption spectra on RRS. Resonance-enhanced Rayleigh scattering is related to scattering located at the molecular absorption band. A comparison between RRS

TABLE 1. Analytical Parameters for the Determination of PUFX

| Method | System | Linearity range ($\mu\text{g mL}^{-1}$) | Regression equation: $C, \mu\text{g mL}^{-1}$ | Correlation coefficient (r) | Detection limit 3σ , (ng mL^{-1}) |
|--------|----------------|---|---|---------------------------------|---|
| RRS | Y(III)-PUFX-EY | 0.004 – 3.0 | $\Delta I = 1020.6 + 1803.2C$ | 0.9989 | 1.1 |
| FQ | Y(III)-PUFX-EY | 1.5 – 7.6 | $\Delta I = -271.57 + 2743.9C$ | 0.9987 | 8.5 |

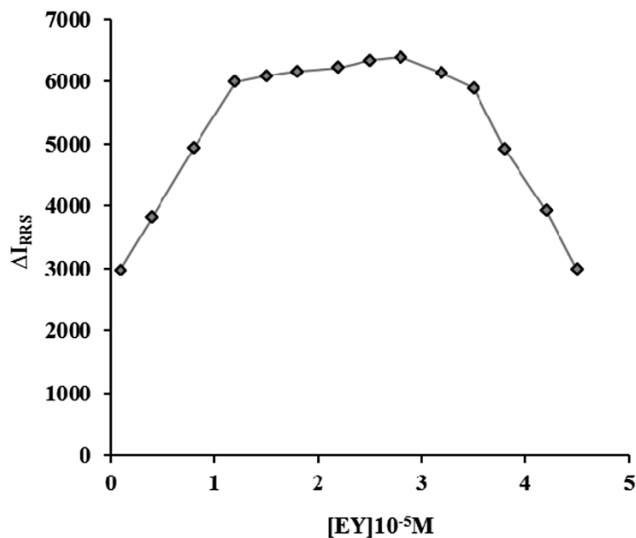


Fig. 5. Effect of EY concentration on I_{RRS} in Y(III)-PUFX-EY system at 375 nm. Concentrations: [PUFX] = 3.0 $\mu\text{g mL}^{-1}$; [Y(III)] = 2.0×10^{-5} M.

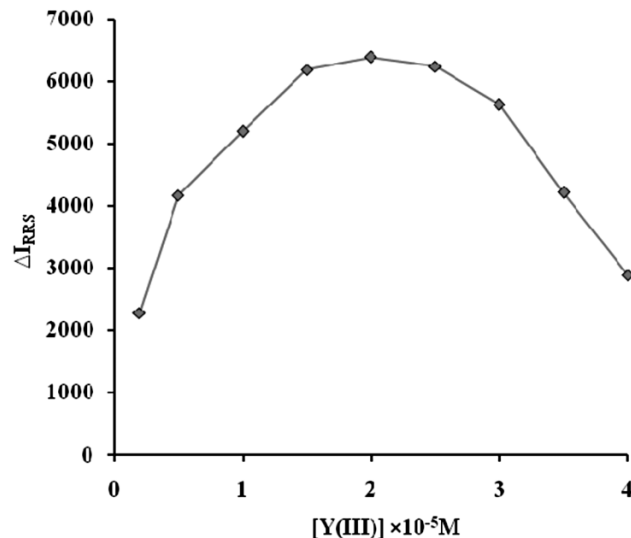


Fig. 6. Effect of Y(III) concentration on I_{RRS} in Y(III)-PUFX-EY system at 375 nm. Concentrations: [PUFX] = 3.0 $\mu\text{g mL}^{-1}$; [EY] = 2.8×10^{-5} M.

spectra and absorption spectra reveals that the RRS peaks occur on the red side of the absorption band of Y(III)-PUFX-EY system and RRS peaks correspond to absorption peaks. The RRS peaks located at 375 nm and 570 nm correspond to absorption peaks located at 350 nm and 530 nm. Although there is some space between RRS peak and absorption peak, the RRS band is still located nearby the absorption band. The probable reasons might be that, when scattering molecules absorb the light energy at

350 nm and 530 nm, the absorption-rescattering process takes place. A small loss of energy during this process imparts the RRS peak a red shift from 350 nm to 375 nm and from 530 nm to 570 nm. As RRS is a special scattering when Rayleigh scattering takes place at or near the absorption band of the scattering molecules, the intensity increases by several orders of magnitude and no longer follows the Rayleigh Law of $I \propto 1/\lambda^4$ [25]. So, the resonance Rayleigh scattering is an important factor in RRS.

TABLE 2. Comparison of Sensitivities of the RRS and Other Methods for the Determination of PUFX

| Method | Analytical reagent | Medium condition | Linearity range | λ_{max} (nm) | LOD | Ref. |
|--------|---|--|---|---|-----------------------------|-----------|
| LC-MS | — | Methanol:water:formic acid (70:30:0.2) | 0.025 – 5.0 $\mu\text{g mL}^{-1}$ | — | 0.025 $\mu\text{g mL}^{-1}$ | [6] |
| CE-CL | Ce(IV)-sulfite-Tb(III) | pH 6.1 | 0.4 – 80 $\mu\text{g mL}^{-1}$ | | 0.084 $\mu\text{g mL}^{-1}$ | [8] |
| SF | Tb(III) | pH 6.5 | 0.032 to 22.56 $\mu\text{g mL}^{-1}$ | $\lambda = 545$ nm | 1.54 ng mL ⁻¹ | [9] |
| SF | PUFX-Tb ³⁺ | | 3.0×10^{-9} to 1.0×10^{-6} g/mL | $\lambda_{\text{ex}}/\lambda_{\text{em}}$ 345/545 | 2.1×10^{-9} g/mL | [10] |
| CL | Cerium(IV)-sulfite-fluoroquinolone-Tb(III) | pH 6.1 | 0.4–80 gm L ⁻¹ | $\lambda_{\text{ex}}/\lambda_{\text{em}}$ 290/545 | 0.084 $\mu\text{g mL}^{-1}$ | [11] |
| CL-FI | KMnO ₄ -Na ₂ S ₂ O ₄ -Tb(III) | pH 5.8 | 9.0×10^{-9} – 5.0×10^{-6} M | λ_{em} 545 | 7.0×10^{-9} M | [12] |
| FQ | Y(III)-EY | pH 6.4 | 1.5 – 7.6 $\mu\text{g mL}^{-1}$ | $\lambda_{\text{ex}}/\lambda_{\text{em}}$ 515/540 | 8.5 ng mL ⁻¹ | This work |
| RRS | Y(III)-EY | pH 6.4 | 0.004 – 3 $\mu\text{g mL}^{-1}$ | 375 | 0.73 ng mL ⁻¹ | This work |

SF: spectrofluorimetry; CL-FI: chemiluminescence–flow injection; CE-CL: capillary electrophoresis-chemiluminescence; LC-MS: liquid chromatography-tandem mass spectrometry; FQ: fluorescence quenching.

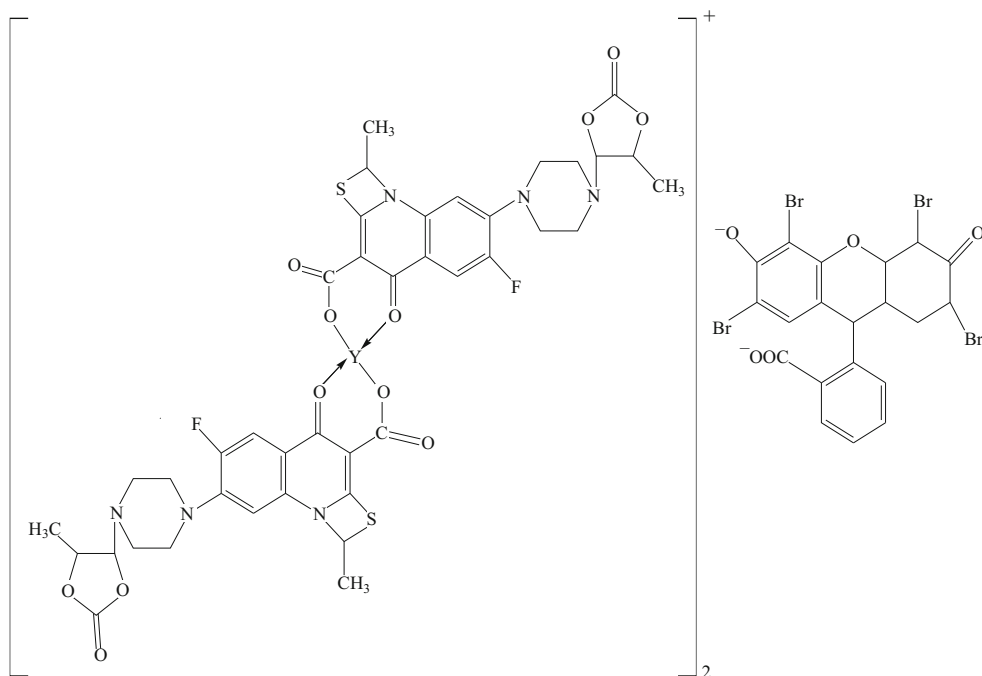


Fig. 7. Possible structures of ternary ion-association complex of PUFX with Y(III) and EY^{2-} .

Effect of hydrophobic surface formation. Before the reaction, EY is doubly negative-charged, while Y(III)–PUFX chelate is cation with one positive charge, and they both are well water-soluble and can form hydrates easily in water. The scattering intensities are very weak under this condition. When they react with each other to form an ion-association complex, their charges are neutralized and they lose hydrophilicity. Therefore, hydrophobic interface forms between the hydrophobic aryl framework of the ion-association complex and aqueous phase. The formation of this hydro-

phobic interface is a favorable factor for the enhancement of scattering [26].

Effect of increased molecular volume. It is known that the bigger the molecular volume, the higher the RRS intensity. Since the molecular volume is not easy to calculate, it can be substituted by molecular weight, i.e., $I = KCM I_0$ [27], where I is the resonance Rayleigh scattering intensity, I_0 is the incident light intensity, C is the solution concentration, K is the proportional coefficient, and M is the molecular weight. Therefore, when K , C , and I_0 are constant, then I is

TABLE 3. Effect of Coexisting Substances ($[PUFX] = 2.0 \mu\text{g mL}^{-1}$)

| Coexisting substances | Concentration ($\mu\text{g mL}^{-1}$) | Change in I_{RRS} (%) | Coexisting substances | Concentration ($\mu\text{g mL}^{-1}$) | Change in I_{RRS} (%) |
|-----------------------|---|-------------------------|--------------------------|---|-------------------------|
| Na^+ | 190 | 1.14 | Fe_2O_3 | 210 | 9.20 |
| K^+ | 310 | 1.36 | β -Alanine | 320 | -2.45 |
| Ca^{2+} | 100 | -4.83 | Glycine | 55 | -2.18 |
| NH_4^+ | 110 | -2.51 | Vit B ₁ | 40 | 2.14 |
| NO_3^- | 90 | -3.55 | β -Cyclodextrin | 320 | -2.42 |
| Cl^- | 320 | -19.9 | Sucrose | 480 | -1.67 |
| Magnesium stearate | 140 | 3.42 | Propylene glycol | 50 | 4.52 |
| Al^{3+} | 60 | 2.73 | Glucose | 280 | -1.87 |
| Ni^{2+} | 150 | 1.45 | Amorphous SiO_2 | 270 | -3.91 |
| Pb^{2+} | 90 | 2.91 | Lactose Monohydrate | 310 | -1.80 |
| Zn^{2+} | 80 | 3.93 | Powdered TiO_2 | 240 | -2.18 |
| Cu^{2+} | 130 | -1.17 | Hypromellose | 220 | 1.82 |

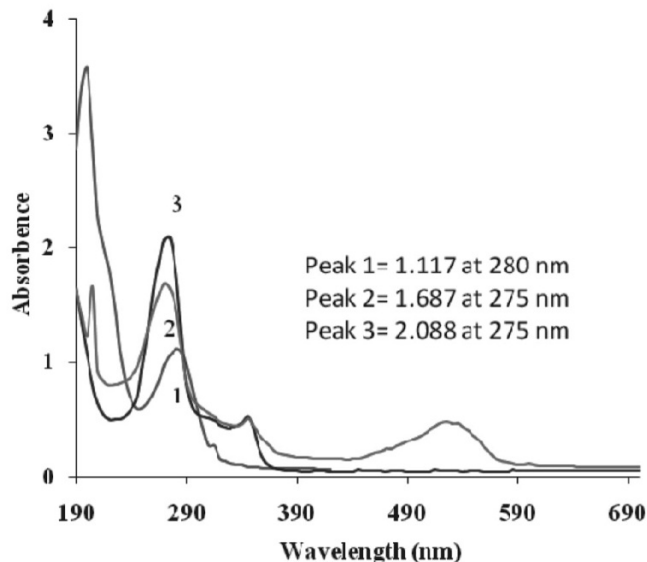


Fig. 8. Absorption spectra of PUFX in various systems. In all spectra, the background absorption was subtracted by using a reference solution (except PUFX, which is being evaluated): (1) PUFX; (2) PUFX–Y(III); (3) Y(III) –PUFX–EY. Concentrations: [PUFX] = $3.0 \mu\text{g mL}^{-1}$; [Y(III)] = 2.0×10^{-5} M; [EY] = 2.8×10^{-5} M.

proportional to M . When the binary chelate $[\text{Y} \cdot \text{PUFX}_2]^+$ reacts with EY^{2-} to form the ternary complex $[\text{Y} \cdot \text{PUFX}_2]_2\text{EY}$, the molecular weights increases from 1011.82 to 2715.54. The increment of the molecular volume (or weight) is a significant factor for the enhancement of RRS intensity.

Energy transfer between absorption, fluorescence and RRS. It can be seen that there is a relationship of ‘as one falls, another rises’ type between the absorbance, fluorescence and RRS intensity. On moving from pure PUFX to ternary ion-association complex of Y(III) and EY, the absorbance decreases and the fluorescence intensity quenches, but RRS enhances notably (Fig. 9). Resonance Rayleigh scattering is a resonance-enhanced scattering produced by the resonance between Rayleigh scattering and ab-

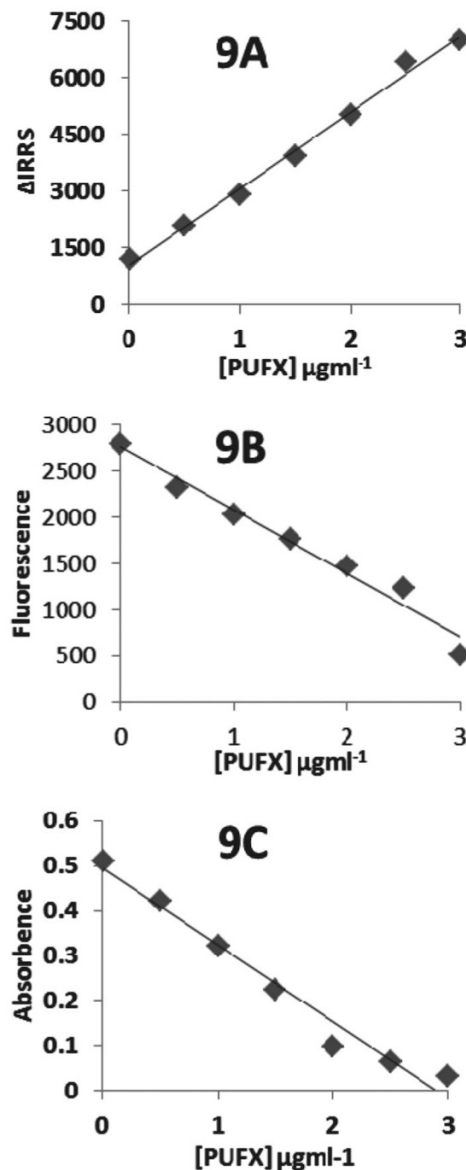


Fig. 9. Relationships between the RRS, fluorescence and absorbance: as the value of ΔIRRS increases, the fluorescence and absorbance values are decreasing.

TABLE 4. Evolution of Accuracy and Precision of Proposed RRS and FQ Methods

| Method | Added ($\mu\text{g mL}^{-1}$) | Found \pm SD ^a ($\mu\text{g mL}^{-1}$) | % Er ^b | (%) RSD ^c | (%) Recovery |
|--------|---------------------------------|---|-------------------|----------------------|--------------|
| RRS | 0.005 | $0.004 \pm 1.1 \times 10^{-4}$ | 0.64 | 2.20 | 99.36 |
| | 0.08 | $0.07 \pm 1.15 \times 10^{-3}$ | 0.40 | 1.44 | 99.60 |
| | 0.50 | $0.50 \pm 1.3 \times 10^{-2}$ | 0.62 | 2.65 | 100.8 |
| FQ | 0.01 | $0.010 \pm 2.7 \times 10^{-4}$ | 0.79 | 2.75 | 100.8 |
| | 1.50 | $1.50 \pm 3.6 \times 10^{-2}$ | 0.26 | 2.42 | 100.3 |
| | 3.20 | $3.23 \pm 7.9 \times 10^{-2}$ | 0.26 | 2.46 | 100.9 |

^a Mean \pm S. D. (for five determinations); ^b Percentage relative error; ^c percentage relative standard deviation.

TABLE 5. Result of Determination of PUFX in Pharmaceutical Samples

| Method | Sample | Label claim (g/tablet) | Found | Mean | % RSD | % Recovery |
|--------|--------|------------------------|--------------------------------------|--------|-------|------------|
| RRS | Ruzilo | 0.600 | 0.601, 0.603, 0.599, 0.597, 0.604 | 0.6010 | 0.485 | 100.2 |
| FQ | Ruzilo | 0.600 | 0.602, 0.606, 0.599, 0.596, 0.605 | 0.6016 | 0.691 | 100.3 |

sorption at the same frequency. During this process, scattering enhances because it absorbs the light energy and part of it is transferred to scattering through the resonance effect. Therefore, as RRS is enhanced, the absorbance decreases. There is a relation between the energy released and energy absorbed. The absorbed light energy (E_A) is equal to the sum of the energy of light emitted (fluorescence) (E_L), resonance scattering (E_{RRS}) and non-radiation (E_N):

$$E_A = E_L + E_{RRS} + E_N.$$

The resonance scattering in transparent solutions of small molecular systems has been seldom studied but the existence of resonance scattering in the large molecule or ion-association systems cannot be ignored. The RRS spectrum lies in its fluorescence band, there would be an energy transfer from fluorescence to resonance scattering. The fluorescence quenching can not be only considered as transfer of the radiation to non-radiation energy, but also as transfer between the fluorescence and resonance scattering. A part of radiant fluorescence is transferred to the resonance scattering through the resonance effect to produce a resonant light scattering. The synchronous change of FQs quenching and RRS enhancement can be seen from Fig. 9. It is a very common phenomenon that FQ can be observed in the study of RRS of fluorescence systems. It is believed that the enhancement of RRS is the consequence of the energy transfer from light absorption and light emission to the scattering [28].

3.7. Selectivity of RRS Method and Its Analytical Application

Effects of coexisting substances. Under optimum conditions, we investigated the effects of some coexisting substances associated with PUFX in the pure form and its formulations using the RRS method developed for the determination of PUFX (Table 3). The influence of foreign coexisting substances, such as metal ions, non-metal ions, amino acids and saccharides, on the determination of 2 $\mu\text{g/mL}$ PUFX was examined. As shown in Table 1, the RRS method can be employed to determine PUFX directly in samples on highly interfering background. So, the RRS method has a good selectivity.

Analytical applications. For determining PUFX in pharmaceutical formulations, various aliquots of PUFX were transferred into 10.0 mL volumetric flasks according to the general procedure. The accuracy and precision of the pro-

posed methods were evaluated by five replicate determinations of PUFX at three different concentrations (Table 4). The results showed that % recovery was in the range of 98.36 – 100.8 and 100.3 – 100.9 with % relative error ranging within 0.402 – 0.644 and 0.266 – 0.928 (for RRS and FQ respectively) reflecting the high accuracy of the proposed procedures, in addition to the high precision as indicated by very low values of % R. S. D. The two methods are therefore recommended for the determination of PUFX in pharmaceutical formulation (Table 5).

4. CONCLUSION

Two new methods for the determination of PUFX were proposed based on the formation of ternary ion-association complex which resulted in enhancement of RRS and quenching fluorescence intensities. The proposed methods are simple, rapid, and highly sensitive and were successfully applied for the determination of PUFX in pharmaceutical samples with satisfactory results. These techniques may also be a valuable approach for the development of PUFX detection in serum and urine samples.

REFERENCES

1. T. Yoshida and S. Mitsuhashi, *Antimicrob. Agents Chemother.*, **37**, 793 – 800 (1993).
2. Y. Okuhama, K. Momota, and A. Morino, *Arzneim. Forsch.*, **47**, 276 – 284 (1997).
3. M. Nakashima, T. Uematsu, K. Kosuge, et al., *J. Pharmacol.*, **34**, 930 – 937 (1994).
4. R. Picollo, N. Brion, V. Gualano, et al., *Arzneim. Forsch.*, **53** (2003) 201 – 205.
5. J. Wen, Z. Y. Zhu, Z. Y. Hong, et al., *Chromatography*, **66**, 37 – 41 (2007).
6. L. X. Guo, M. L. Qi, X. Jin, et al., *J. Chromatogr. B*, **832**, 280 – 285 (2006).
7. A. T. Luo, H. F. Liu, X. K. Wang, and H. Li, *Memoirs*, **3**, 31 – 33 (2006).
8. Z. Yang, X. Wang, W. Qin, and H. Zhao, *Anal. Chim. Acta*, **623**, 231 – 237 (2008).
9. F. Yu, F. Chen, S. Zheng, and L. Chen, *Anal. Lett.*, **41**, 3124 – 3137 (2008).
10. T. Wu, B. Fang, L. Chang, et al., *Luminescence*, **28**, 894 – 899 (2013).
11. Z. Yang, X. Wang, W. Qin, and H. Zhao, *Anal. Chim. Acta*, **623**, 231 – 237 (2008).

12. M. Cui, F. Yu, F. Chen, and L. Chen, *Anal. Lett.*, **41**, 2001 – 2012 (2008).
13. X. L. Wang, A. Y. Li, H. C. Zhao, and L. P. Jin, *J. Anal. Chem.*, **64**, 75 – 81 (2009).
14. C. Z. Huang, K. A. Li, and S. Y. Tong, *Anal. Chem.*, **68**, 2259 – 2263 (1996).
15. C. Q. Ma, K. A. Li, and S. Y. Tong, *Anal. Biochem.*, **239**, 86 – 91 (1996).
16. S. P. Liu, H. Q. Luo, N. B. Li, and Z. F. Liu, *Anal. Chem.*, **76**, 3907 – 3914 (2001).
17. S. P. Liu, Z. F. Liu, and H. Q. Luo, *Anal. Chim. Acta.*, **12**, 255 – 260 (2000).
18. M. Oshima, N. Goto, J. P. Susanto, and S. Motomizu, *Analyst*, **121**, 1085 – 1088 (1996).
19. S. P. Liu, S. Chen, Z. F. Liu, et al., *Anal. Chim. Acta*, **535**, 169 – 175 (2005).
20. X. Q. Wei, Z. F. Liu, and S. P. Liu, *Anal. Biochem.*, **346**, 330 – 332 (2005).
21. X. L. Hu, S. P. Liu, and N. B. Li, *Anal. Bioanal. Chem.* **376**, 42 – 48 (2003).
22. S. H. Fu, Z. F. Liu, S. P. Liu, et al., *Anal. Chim. Acta*, **599**, 271 – 278 (2007).
23. Z. Jiang, R. Cai, and H. Zhang, in: *Analytical Chemistry of Rare Earths*, 2nd ed., Science Publishing: Beijing (2000), pp. 21 – 30.
24. N. El-Enany, *Il Farmaco*, **59**, 63 (2004).
25. S. G. Stanton, R. Pecora, and B. S. Hudson, *J. Chem. Phys.*, **75**, 5615 – 5626 (1981).
26. S. P. Liu and L. Kong, *Anal. Sci.*, **19**, 1055 – 1060 (2003).
27. *Chinese Macropaedia Biology (II)*, Chinese Macropaedia Press, Beijing (1991), p. 1374.
28. X. L. Tang, Z. F. Liu, S. P. Liu, and X. L. Hu, *Sci. Chin. Ser. B*, **50** 54 – 62 (2007).